Exploring process-level genotypic and environmental effects on sugarcane yield using an international experimental dataset

Jones MR[1,2,*], Singels A[1,2], Chinorumba S[3], Patton A[1], Poser C[4], Singh M[5], Martiné JF[4], Christina M[4], Shine J[5], Annandale J[2], Hammer G[6].

[1]South African Sugarcane Research Institute, Private Bag X02, Mount Edgecombe, 4300, South Africa

[2]Department of Plant and Soil Sciences, University of Pretoria, Private Bag X20, Hatfield, 0028, South Africa

[3] Zimbabwe Sugar Association Experiment Station (ZSAES), P. Bag 7006, Chiredzi, Zimbabwe.

[4] Centre de Coopération Internationale en Recherche Agronomique pour le Développement (CIRAD), Persyst UPR SCA, Station de La Bretagne - BP 20, F97408 Saint-Denis, Messagerie Cedex 9, La Réunion (France)

[5]Sugarcane Industry Research Committee (SIRC), c/o Sugarcane Growers Cooperative of Florida, 1500 George Wedgworth Way, Belle Glade, Florida 33430, USA.

[6]ARC Centre of Excellence for Translational Photosynthesis, Queensland Alliance for Agriculture and Food Innovation, The University of Queensland, Brisbane, Qld 4072, Australia

*Corresponding author: Matthew Jones (matthew.jones@sugar.org.za).

Highlights

- An international G by E sugarcane growth analysis dataset was collected
- E and GxE variation were present in final dry biomass and stalk yields
- G differences found for germination, canopy development and photosynthesis parameters
- Data analysis reveals strengths and weaknesses in process model concepts
- Solar radiation, in addition to temperature, influences onset of stalk growth

Abstract

Crop improvement aims to produce high yielding genotypes for target environments. Crop models simulate yield formation as the outcome of a series of low-level processes, driven by environmental (E) variables and regulated by genetic (G) traits. There is potential for crop models to aid sugarcane breeding, by identifying desirable genetic traits for target environments. The objective of this study was to evaluate existing concepts of G and E control of plant processes for explaining crop development, growth and yield, using an international growth analysis dataset.

Crop development, growth and yield were monitored in the plant and 1st ratoon crops for seven cultivars (N41, R570, CP88-1762, HoCP96-540, Q183, ZN7 and NCo376) grown under well-watered conditions at La Mare (Reunion Island, France), Pongola (South Africa (RSA), Chiredzi (Zimbabwe), and Belle Glade (Florida, USA). Weather data were collected and environmental conditions characterized for each experiment. Derived process-level phenotypic parameters, based on concepts from four sugarcane growth simulation models (DSSAT-Canegro, Mosicas, APSIM-Sugar and

Canesim), were calculated from observations and used to (1) evaluate current understanding of E drivers of sugarcane growth and development processes, and (2) identify and quantify G control at a process level.

Final yields showed significant E and GxE variation; dry above-ground biomass and stalk yields were highest in La Mare and lowest in Pongola. Cultivar rankings in stalk dry mass for the common cultivars (N41, R570, CP88-1762) varied significantly between Es. Significant E variation in phenotypic parameters describing germination, tillering and timing of the onset of stalk growth (OSG) revealed shortcomings in the underlying simulation concepts. Significant G variation was found for germination rate, leaf appearance rate and canopy development rate per unit thermal time (TT), and maximum radiation use efficiency, indicating strong G control of the associated underlying processes.

Solar radiation was found to influence tillering rate per unit TT, and TT to OSG, challenging the current theory of TT as the sole driver of these processes.

By explaining more of the E variation, more stable and accurate G-specific model parameters can be defined and evaluated. This is anticipated to lead to less GxE confounding of modelled processes, and hence crop models that are better-equipped for supporting sugarcane crop improvement.

Keywords: Crop model, thermal time, tillering, canopy development, environment, genotype, growth

INTRODUCTION

Sugarcane is an important crop worldwide, as a sweetener, source of dietary calories, and feedstock for bioenergy production. In 2017 about 1.84 billion tons of cane were produced from 25 million ha in more than 100 countries in the tropical and subtropical regions of the world (FAO, 2019). Major producers include Brazil, India, China, Thailand, Pakistan and Mexico. Sugarcane production also makes vital contributions to national economies of smaller producers, such as Australia and several African countries.

Many of these industries invest substantially in breeding cultivars well-adapted to local environmental conditions and field management.

Crop models have potential to assist sugarcane breeding by identifying desirable traits for target environments. Models can be used to dissect high-level complex traits (such as yield at harvest) to isolate and characterise E and G control over lower level traits (such as photosynthetic efficiency or leaf expansion rate). Crop models suitable for such applications are required to be strongly process-based, where complex trait values emerge as a consequence of process-level interactions with G (represented by G-specific model parameters) and E control (represented by climatic input variables, simulated soil water and nutrient balances and management related inputs) (Hammer and Jordan, 2007; Yin et al., 2004).

Crop models represent quantitative syntheses of objective knowledge of crop physiological processes (Boote et al., 2010). Assessing crop model process concepts against experimental data could reveal the extent to which current knowledge adequately captures G and E control at a process level. Possible weaknesses in

process concepts and assumptions could be identified that need attention for sugarcane crop models to become suitable for breeding applications. Analyzing crop model concepts outside of the models permits clearer process-level evaluation, because doing so eliminates any potentially confounding effects from other parts of the models.

Several process-based sugarcane models have been developed. These include DSSAT-Canegro, “Canegro” (Inman-Bamber, 1991; Jones and Singels, 2018; Singels et al., 2008; Singels and Bezuidenhout, 2002); Canesim (Singels and Donaldson, 2000; Singels and Paraskevepoulos, 2017), a simplified version of Canegro; Mosicas (Martiné et al., 1999; Martiné and Todoroff, 2004); and APSIM-Sugar, “Apsim” (Keating et al., 1999). These models operate on a daily time-step, and simulate germination, canopy development and radiation interception, photosynthesis and biomass accumulation, and biomass partitioning processes to translate G, E and M inputs into predictions of stalk and sucrose yields. There are substantial differences in the model philosophies, which are reflected in differences in the nature of model input parameters and the complexity and approach of constituent process algorithms. The Canegro and Apsim models are used extensively worldwide (Jones et al., 2014; Marin et al., 2013; Thorburn et al., 2014), while use of the Mosicas and Canesim models has been mostly restricted to their industries of origin. The best reported performance of these models is prediction accuracy of approximately 5-7 t/ha for stalk dry mass. (Jones and Singels, 2018).

Sugarcane yield sensitivity to Apsim model cultivar parameters has been assessed by Sexton et al. (2017) for two environments in Australia. Trait modelling in sugarcane has also been explored for drought tolerance, again using the Apsim model (Inman-

Bamber et al., 2016). Site x cultivar effects for several process-level parameters (relating to tillering and stalk elongation) from the Canegro model were statistically assessed by Ngobese et al. (2018), for 12 South African cultivars at two sites (one rainfed, one irrigated). No attempt was made to explain differences in terms of E differences at each site. Parameters that were not stable between sites or crop classes (i.e. plant/ratoon crops) were considered unsuitable for use in breeding applications, rather than evidence of unresolved GxE interactions in the underlying model concepts. Hoffman et al. (2018) calculated Canegro model parameter values for 14 genotypes in a well-watered pot trial, and found significant differences in leaf-level photosynthesis rates, thermal time from primary shoot emergence to the onset of stalk growth, and stalk partitioning fraction. The Canesim model was able to simulate cultivar differences in yield using these independently-determined parameter values for well-watered field conditions (Singels et al., 2016).

Marin et al. (2015) compared simulations from the Canegro and Apsim models and explained simulation differences in terms of detailed descriptions of the process-level algorithms, in the context of climate change impacts simulations. However, as far as we could ascertain Canegro and Apsim (and Mosicas) have not been compared at conceptual process-level with equivalent inputs and assumptions for assessing G, E, and GxE effects.

Operational application of crop models to assist sugarcane breeding activities around the world requires careful evaluation of existing sugarcane models. Testing and comparing process-level algorithm concepts against an appropriate multiple-G, multiple-E trial will reveal strengths and weaknesses of different modelling

approaches, as well as reveal knowledge gaps that limit the effectiveness of sugarcane models in breeding applications.

The overall aim of this study was to characterise crop development and growth observed in an international multi-environment cultivar trial, to gain a better understanding of genotypic and environmental controls of sugarcane crop performance under non-limiting water and nutrient conditions. Avoiding confounding effects of water and nutrient stresses allows a first-step 'potential production' level analysis, and could better reveal subtle genetic effects on crop development and growth.

The specific objectives of this paper were to:

1. Characterise the growth environments in terms of radiation, temperature and water status;
2. Characterise/describe crop development and growth for different G and E.
3. Evaluate current theories/understanding of G and E control of sugarcane development and growth by deriving key parameters for each G-E combination:
4. Thermal time requirements for phenological events, and leaf, tiller and canopy development;
5. Radiation use efficiency; and
6. Biomass partitioning
7. Propose new concepts for G and E control of crop development and growth.
8. Assess the value of the dataset for the broader objectives of unravelling GxE influences on yield, and make recommendations for improving experimental protocols for future studies.

We present an overview of process-level simulation concepts from four mature sugarcane models. The methods section then describes the experiments conducted, how the experimental growth environments were characterised, and how each G-E combination was phenotypically characterised in terms of key simulation concepts. Results are then shown, and discussions and conclusions presented. A table of acronyms is shown below (Table 2) to guide the reader.

SUGARCANE MODEL CONCEPTS

An overview of key processes simulated by the four sugarcane crop models (Canegro, Canesim, Apsim and Mosicas), and how they might be tested against experimental data, is presented in this section. Two versions of the Canegro model are considered: v4.5 (Singels et al., 2008), Canegro1; and v4.5_C2.2 (Jones and Singels, 2018), Canegro2. For simulated processes where these do not differ, “Canegro” is used. The discussion focusses on well-watered and well-nourished sugarcane production.

2.1. Germination

During germination, underground buds sprout shoots that elongate to emerge above the soil surface. The date of shoot emergence (DAP_EM, d) is defined in the Canegro1, Canesim, Mosicas and Apsim models as the date when 50% of primary shoots have emerged (DAP_EM50, d). The Canegro2 model considers shoot emergence as the date when the first shoot emerges (DAP_EM1, d).

All models use air temperature within specific ranges (effective temperature) as the sole E driver of germination rate (and rates of several other plant processes). This is captured in the crop models with the concept of thermal time (TT, °Cd), making use of

a base temperature (T_B, °C), and in the Canegro2, Canesim, Mosicas and Apsim models, optimal (T_O) and upper limit (T_U) cardinal temperatures (Jones and Singels, 2018). These cardinal temperatures are process-specific in Canegro, Canesim and Mosicas, and fixed in Apsim.

Canegro, Canesim and Mosicas predict DAP_EM using TT elapsed since crop start (TT_EM50, °Cd). Apsim simulates a TT delay for bud sprouting, followed by TT-driven shoot elongation from the bud to the soil surface, accounting for the effect of planting depth. All three models differentiate between plant (P) and ratoon (R1) crops for calculating DAP_EM. TT_EM50 is G-specific in Canegro, Canesim and Mosicas.

As all models effectively simulate germination as a function of TT, it is appropriate to evaluate the concept in these terms.

2.2. Canopy development and light interception

Green leaf area index (GLAI, m^2/m^2) determines the fraction of incident solar radiation intercepted for photosynthesis, and affects rates of transpiration and soil evaporation.

All models use the concept of fractional interception (Fi, %) of radiation. Fi of photosynthetically-active solar radiation (PAR, $MJ/m^2/d$) is FiPAR (%), and of global radiation (SRAD, $MJ/m^2/d$), FiSRAD (%).

The Canegro, Apsim and Mosicas models estimate Fi from GLAI, using a radiation extinction coefficient using Beer's Law. The Canesim model simulates FiPAR directly as a function of TT since TT_EM50, with a single G-specific parameter, TT_Fi50 (thermal time from emergence to 50% FiPAR).

The Mosicas model calculates the daily change in unstressed GLAI using a Gompertz derivative equation of TT accumulation since emergence. Apsim and Canegro

calculate GLAI per shoot, where: leaf number (G-specific) is determined by TT via phyllocron intervals (PI, °Cd); area per leaf is determined by leaf number (G-specific), and TT; total green leaf area per shoot is multiplied by shoot population (POPN, shoots/m^2). Leaf area growth in the Apsim model is driven by temperature and limited by water stress in a conceptually similar manner to Canegro, but also requires that sufficient carbohydrate is supplied to the leaves (via biomass accumulation (photosynthesis) and partitioning processes) to support the daily increase in leaf area. Demand for leaf biomass is based on the daily leaf area increase and specific leaf area, which is permitted to vary within bounds. Insufficient biomass results in limits on leaf area expansion. It should be noted that the size of green leaf canopy is not determined by carbohydrate supply (source strength) in Canegro, Canesim and Mosicas. Both Canegro and Apsim effectively simulate TT-driven POPN development, with G-specific control parameters. Canegro2 differentiates between primary and secondary shoots and adjusts tillering rates in response to light competition.

All models are sensitive to water status: Canesim transiently reduces Fi; Mosicas reduces the daily leaf expansion; Canegro and Apsim reduce leaf elongation rates and accelerate leaf senescence rates; and Canegro reduces tillering rates and accelerates shoot senescence rates.

All models make provision for G-specific control over canopy development rates, and the key E determinants of canopy development rate are TT and water stress. For the purposes of evaluating model concepts under unstressed Es, it is adequate to frame, as G-controlled functions of TT since DAP_EM50: (1) canopy development in terms

of FiPAR development rate; and (2) its components, shoot and leaf development, as shoot (tiller) appearance rate and PI respectively.

2.3. Biomass accumulation

Canegro, Canesim, Mosicas and Apsim all simulate biomass accumulation (ΔDM, t/ha/d) using a radiation-use efficiency (RUE) approach (Singels, 2013). RUE can be calculated by dividing observed above-ground dry biomass (ADM) production by measured canopy-intercepted solar radiation. All models calculate daily simulated RUE based on a theoretical maximum RUE value (RUEo, maximum dry biomass produced per unit of canopy-intercepted radiation at optimal temperature, crop water and nutrient status for a young, healthy crop, g/MJ), and air temperature and water status. The Apsim model additionally considers the simulated nitrogen status of the crop. RUE is not affected by radiation intensity in any of these models (i.e. simulated RUE does not decrease under very high radiation conditions).

Canegro, Canesim and Mosicas express RUEo in terms of PAR (assumed in this paper to be 50% of SRAD), while Apsim uses SRAD. Respiration is explicitly simulated by Canegro, Canesim and Mosicas, and not by Apsim. Canegro and Canesim assume the same RUEo for P and R1 crops, while Mosicas and Apsim allow different parameter values for plant and ratoon crops. RUEo is G-specific in Canegro, Canesim and Mosicas, and is considered fixed in Apsim.

Figure 1 shows the RUE relationship with temperature for well-watered crops as used in the different models, using their default input parameter values. The values are expressed according to a common RUEo definition, for meaningful comparison; the

Apsim definition (expressed in g ADM per MJ SRAD) is used as it is the only definition that can express parameter values equivalently for all models.

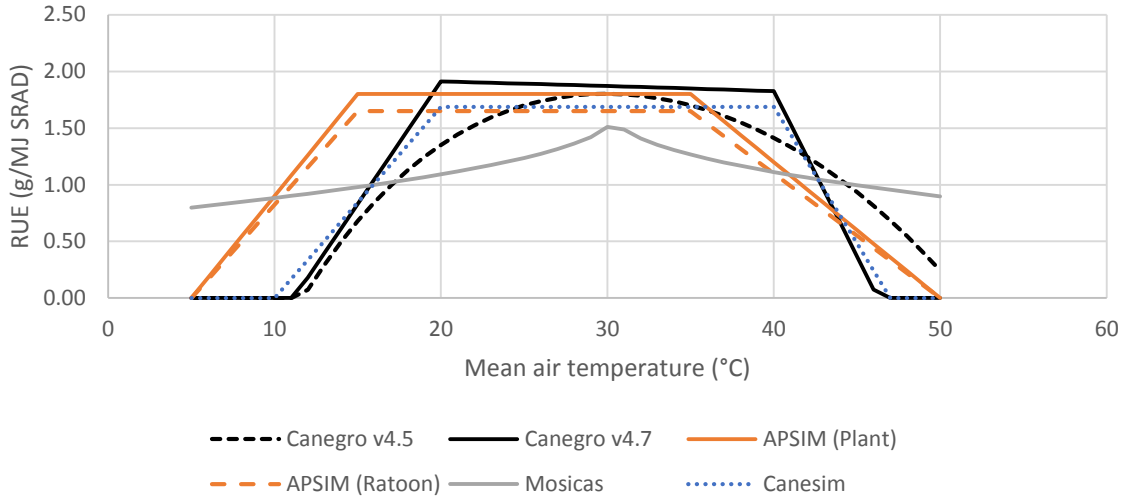

***Figure 1**. Well-watered radiation use efficiency (RUE, g of dry aboveground biomass per MJ of intercepted shortwave solar radiation (SRAD)), for four models, under reference conditions (total biomass = 41 t/ha; stalk dry mass = 18 t/ha; age = 9 months; SRAD = 25 MJ/m^2; unstressed water status) with default model parameter values. RUEo (representing the maximum theoretical RUE values (g/MJ)) are reflected where RUE values are highest.*

Calculating a value for RUEo from observed data is practically difficult, due to the necessity to create RUE-maximising environmental conditions for a sustained period. Analysis of high values of RUE (based on observed ADM and intercepted PAR measurements) for unstressed, healthy crops (RUEmax, g/MJ) could inform understanding of G control over RUEo.

2.4. Biomass partitioning

Canegro, Canesim and Apsim consider onset of stalk growth (OSG) as a phenological event determined solely by TT accumulation after DAP_EM50 (TT_OSG, °Cd;

Singels, 2013), while Mosicas uses an ADM threshold (ADM_OSG, t/ha). As ADM accumulation (ΔADM) is reduced by water stress, Mosicas effectively considers source strength (and water stress) in simulating OSG. These two approaches need to be evaluated separately against observed TT and ADM respectively.

Canegro and Mosicas partition ΔDM between roots (ΔRDM, t/ha/d) and above-ground (ΔADM, t/ha/d) parts as functions of total biomass and crop class. In Apsim, ΔRDM is calculated from ΔADM via growth stage-based multiplier parameters.

Canegro calculates a temperature-sensitive (≈10-17 °C range) STKPF from a reference G-specific parameter (Singels et al., 2005a). Mosicas estimates STKPF as a continuous function of ADM, with a G-specific maximum value and a crop class-specific attenuation coefficient. Apsim considers STKPF to be a fixed G-specific parameter. Default parameter values for the different models are in the range 0.70-0.75 t/t.

STKPF can be evaluated from observed SDM and ADM.

METHODS

This section describes the methodology followed to achieve the stated objectives. A set of experiments is described, followed by a description of analyses conducted to characterise the growth environments in each experiment. We then describe how each G-E combination was phenotyped in terms of process-level model concepts identified in Section 3. Finally, we explain how we assessed the variation in these phenotypic parameters in order to assess E, G and GxE interaction effects. This

allowed us to infer the extent to which G control is exerted at a process level, as well as identify significant remaining E variation that pointed to model concept deficiencies.

3.1. Experiment details

Eight experiments (Es; 'E' is used interchangeably to refer to experiments and environments in this paper) were conducted, consisting of plant and first ratoon crops at sites in four countries (Table 1). The intention was to have the same set of cultivars (genotypes, Gs) grown at all sites, with no water or nutrient limitations. In practice, three Gs were common to all sites (N41, R570 and CP88-1762) and additional Gs (HoCP96-540, Q183, ZN7 and NCo376) were included at some sites, and water stress could not be avoided in some cases. At all sites, expect in Chiredzi, Zimbabwe, two adjacent blocks, A and B, were established at each site. Plant crops were established on both blocks simultaneously, but only the plots in block A were sampled during the first season of growth (recording data for the plant crop). Block B was cut back on the day of the final harvest of block A, and was sampled during the second season of growth (recording data for the first ratoon crop). At Chiredzi, the ratoon crop was started on a different field with a different soil, six months after the harvest date of the plant crop.

Each experiment was designed as a randomised complete block with five plots per treatment; each plot consisted of 9 rows of 11 m long, spaced at 1.5 m. Non-destructive measurements of top visible dewlap height (TVDH, cm) and leaf number (tagged shoots), and shoot population (2 m row-length), were conducted every one to four weeks, with more frequent sampling during the partial canopy and tillering phases. Destructive samples (of 18 m^2) were taken on four occasions – 3, 6, 9 and 12 months' age. Leaf area, shoot and leaf counts, and fresh and dry biomass fractions were

***Table 1**. Experimental details. All experiments included cultivars N41, R570 and CP88-1762.*

Country, site and location	Additional cultivars	Crop class	Start date	Harvest date	Irrigation type	Soil type	Notes
Reunion, La Mare. 20°57'0"S; 55°18'0"E; 70 m a.s.l.	Q183, NCo376	Plant	2015-02-25	2016-02-23	Overhead sprinkler	Hypereutric Nitisols	Irrigation suspended after 3 months in plant crop.
		Ratoon	2016-01-18	2017-01-25			
South Africa, Pongola. 27°24'0"S; 31°35'0"E; 308 m a.s.l.	HoCP96-540, HoCP96-540, ZN7	Plant	2014-03-25	2015-03-24	Overhead sprinkler and drip	Rhodic Cambisol	Limited irrigation in ratoon crop.
		Ratoon	2015-03-24	2016-03-23			
USA, Belle Glade. 26°39'02"N; 80°38'08"W; 5 m a.s.l	NCo376, Q183, HoCP96-540	Plant	2013-12-12	2015-01-04	Water table	Dystric Sapric Histosol	
		Ratoon	2015-01-23	2016-01-26			
Zimbabwe, Chiredzi. 21°02'01.95"S, 31°36'58.52"E, 420 m a.s.l.	Q183, HoCP96-540, ZN7	Plant	2013-10-30	2014-11-26	Furrow	Eutric Luvisol	Plant and ratoon crop fields not adjacent in space or time
		Ratoon	2015-06-03	2016-06-03	Floppy overhead sprinkler	Eutric Luvisol	

***Table 2**. Symbols, their units and meanings.*

Acronym	Units	Description
ADM	t/ha	Above-ground dry biomass
ADM_OSG	t/ha	ADM on date of onset of stalk growth
Apsim		APSIM-Sugar
cv%	%	Coefficient of variance
DAP_EM	d	Days from crop start to primary shoot emergence
DAP_EM50	d	Days from crop start to 50% primary shoot emergence
Canegro		DSSAT-Canegro
Canegro1		DSSAT-Canegro v4.5
Canegro2		DSSAT-Canegro v4.5_C2.2
E		Environment or experiment
Fi	%	Fractional interception of radiation
FiPAR	%	Fractional interception of PAR
G		Genotype or cultivar
GLAI	m^2/m^2	Green leaf area index
IntPAR	MJ/m^2	Intercepted PAR
Mosicas		Mosicas
OSG		Onset of stalk growth (phenological event)
P		Plant crop
PAR	MJ/m^2	Photosynthetically-active radiation
PFINAL	$shoots/m^2$	Final shoot population
PI	°Cd/leaf	Leaf phyllocron interval
POPN	$shoots/m^2$	Shoot population
PPEAK	$shoots/m^2$	Peak shoot population
PTQ	$MJ/m^2/°Cd$	Photothermal quotient

PTQc	$MJ/m^2/°Cd$	Cumulative daily PTQ
PTQd	$MJ/m^2/°Cd$	Daily PTQ
R1		First ratoon crop
RUE	g/MJ	Radiation use efficiency (photosynthetic conversion efficiency) calculated as the aboveground dry biomass produced over a given period divided by PAR intercepted over the same period
RUEmax	g/MJ	Maximum observed RUE calculated over four biomass sampling periods
RUEo	g/MJ	Theoretical maximum RUE under ideal conditions (optimal temperature, water status and nutrient status)
SDM	t/ha	Stalk dry mass
SRAD	MJ/m^2	Global solar radiation
STKPF	t/t	Stalk partitioning fraction
TAR	$shoots/m^2/°Cd$	Tiller appearance rate per unit TT
T_B	°C	Base temperature for thermal time accumulation
TMAX	°C	Maximum daily air temperature
TMIN	°C	Minimum daily air temperature
T_O	°C	Optimal temperature for thermal time accumulation
TT	°Cd	Thermal time
TT_EM50	°Cd	TT from crop start to 50% primary shoot emergence
TT_Fi50	°Cd	TT from TT_EM50 to 50% FiPAR
TT_OSG	°Cd	TT from DAP_EM50 to date of OSG
TT10	°Cd	TT calculated with Canegro2 cardinal temperatures for leaf elongation

TT16	°Cd	TT calculated with Canegro2 cardinal temperatures for tillering
TT9	°Cd	TT calculated with Apsim cardinal temperatures
T_U	°C	Upper temperature for thermal time accumulation
WSI		Water stress index
ΔADM	t/ha/d	Daily change in ADM
ΔADMp	t/ha	Change in ADM for period p
ΔIntPARp	MJ/m^2	Change in intercepted PAR for period p
ΔRDM	t/ha/d	Daily change in root dry mass

determined based on 3 m^2 sub-samples. Dry mass values for biomass components (e.g. ADM and SDM) were determined by multiplying the respective dry mass fractions (calculated using the 3 m^2 sub-samples) by the 18 m^2 above-ground fresh mass samples. Radiation interception by the canopy was measured non-destructively, using handheld line quantum sensors, on several occasions throughout each crop. Departures from this basic protocol are highlighted in the results. Some other limitations were noted for certain crop and genotype combinations. These are noted in the results.

3.2. Environmental characterisation

3.2.1. Thermal time

Cumulative TT was calculated as described by Jones and Singels (2018). TT9 used Apsim cardinal temperatures (T_B = 9, T_O = 32, T_U = 45 °C); TT10 and TT16 used Canegro2 cardinal temperatures for leaf development (T_B = 10, T_O = 30, T_U = 43 °C) and tiller development (16, 35, 48 °C) respectively.

3.2.2. Crop water status

The water stress index (WSI) was calculated as the cumulative sum of daily photosynthesis water stress (SWDF2) values simulated by the Canegro2 model, using standard cultivar coefficients.

3.2.3. Photo thermal quotient

The photo-thermal quotient (PTQ, Nix, 1976) is the ratio of solar radiation to TT accumulation, and captures the combined effect of radiation as the primary source of carbon accumulation and temperature as a main carbon sink determinant. This concept has been used to explain variation in tillering in sorghum (Kim et al., 2010) but has not been used in sugarcane models.

Daily cumulative PTQ (PTQc, MJ/m^2/°Cd) is reported for the environmental characterisation, and was calculated as:

$$PTQ_c = \sum_{d=1}^{D} \min(6, PTQ_d) \quad (2)$$

$$PTQ_d = \frac{SRAD}{TT10} \quad (3)$$

Daily PTQ (PTQ_d, MJ/m^2/°Cd) was limited to 6 MJ/m^2/°Cd, based on analysis of the PTQd values (mean = 2.15, median = 1.38 MJ/m^2/°Cd; excluded outliers amounted to < 1 % of the dataset). This was to avoid PTQ_d reaching enormous values on days where the air temperature is near or below the base temperature of 10 °C. PTQ_c values were used visually (only).

3.3. Phenotypic characterisation

Descriptive phenotypic parameters were calculated either directly or derived from observed data. The derived parameters are based on concepts from the different models, and the focus was on parameters understood to be of particular importance to these models.

3.3.1. Canopy development

Methods for calculating values for TT_EM50, PI, tiller appearance rate per unit thermal time (TAR, shoots/m^2/°Cd), peak shoot population (PPEAK, shoots/m^2), final shoot population (PFINAL, shoots/m^2), TT_Fi50, seasonal intercepted PAR (IntPAR, MJ/m^2) and seasonal average FiPAR (FiPARavg, %) are described in this section.

- TT_EM50 was calculated as the cumulative TT10 value on the date of DAP_EM50 (preliminary analysis showed little difference between TT measures calculated with different cardinal temperatures). DAP_EM50 is required to estimate TT_EM50, and had been observed for the Reunion P and Belle Glade P and R1 crops. In other cases, DAP_EM50 was inferred from POPN observations (methodology explained in Section 1.3 of the Supplementary Online Material).
- PI was calculated as the inverse of leaf appearance rate per unit thermal time (LAR0, leaves/shoot/°Cd). LAR0 was calculated as the slope of the linear regression of total leaf number per shoot (TLFN) against TT10, for TT10 values less than 3100 °Cd.
- TAR was calculated as the slope of the linear regression of POPN against TT16, from DAP_EM50 to date of PPEAK.

- PFINAL was estimated from the last three POPN observations.
- PPEAK was taken as the maximum observed (treatment mean) POPN value.
- TT_Fi50 was used to characterize canopy development. Values were estimated by optimising the Canesim FiPAR model (see Supplementary Online Material) parameters to achieve a good fit to FiPAR observations. A genetic algorithm ("Genoud", Mebane and Sekhon, 2011) was used for parameter optimisation. TT_Fi50 could not be determined for Chiredzi R1 due to lack of reliable data.
- IntPAR was calculated as the dot-product of fitted daily FiPAR (from the Canesim model) and PAR values.
- FiPARavg was calculated as the ratio of IntPAR to total seasonal incident PAR, expressed as a percentage.

3.3.2. Biomass accumulation and partitioning

ADM, SDM and IntPAR data were used to estimate parameters for biomass accumulation (RUEmax, defined as the maximum RUE observed in all biomass sampling periods) and partitioning (ADM_OSG, TT_OSG and STKPF).

- RUEmax was calculated as highest of RUE calculated per biomass sampling period p (RUE_p, g/MJ)

$$\mathrm{RUE_p} = \frac{\Delta \mathrm{ADM_p} * 100}{\Delta \mathrm{IntPAR_p}} \quad (5)$$

where ΔADM_p (t/ha) and $\Delta IntPAR_p$ (MJ/m^2) are the changes in ADM and IntPAR between consecutive sampling dates.

- ADM_OSG was determined by linearly regressing SDM (> 0 t/ha) against ADM and then finding the x-intercept. TT_OSG was taken as the TT10 age since

DAP_EM50 at which ADM = ADM_OSG. For Chiredzi R1 only, TT_OSG was additionally estimated using TVDH (top visible dewlap height, a measure of plant height, cm) data, as the ADM_OSG values appeared too high for this E. TVDH was regressed against TT16, and the corresponding TT10 value (since DAP_EM50) when TVDH was last projected to be zero was taken as TT_OSG.

- STKPF was calculated as the slope of linear regression of SDM and ADM.

3.3.3. Analysis of variance

ANOVA was conducted on ADM and SDM final values using the R 'aov' function for analysis of variance (R Core Team, 2016).

For each phenotypic parameter, the mean and standard deviation of E values for each G were calculated: E variation was quantified as the standard deviation of E means (averaged over Gs), divided by the overall (averaged over Es) mean value, expressed as a percentage (Ecv, Eq. (6)). An Ecv value exceeding 25% was taken as an indication of strong E impact.

$$Ecv = \frac{stddev(MV_{E1}, MV_{E2}, \dots, MV_{En})}{mean(MV_{E1}, MV_{E2}, \dots, MV_{En})} * 100 \quad (6)$$

$$MV_{Ey} = mean\left(Value_{Ey,G1}, Value_{Ey,G2}, Value_{Ey,G3}\right) \quad (7)$$

where MV_{Ey} is the mean phenotypic parameter value ($Value_{E,G}$) for the three common Gs (G1, G2, G3) for environment y (Ey).

Similarly, the mean and standard deviation of G values for each E were calculated: G variation was quantified as the standard deviation of G means (averaged over Es), divided by the overall (averaged over Gs) mean value, expressed as a percentage (Gcv, Eq. (8)). In addition the variation in G rankings was quantified as the standard

deviation of average G rankings across Es, divided by the mean G ranking, expressed as a percentage (GRcv, Eq. (10)). G impacts were considered strong when Gcv exceeded 8% and GRcv exceeded 25%.

$$Gcv = \frac{stddev(MV_{G1}, MV_{G2}, MV_{G3})}{mean(MV_{G1}, MV_{G2}, MV_{G3})} * 100 \quad (8)$$

$$MV_{Gx} = mean\left(Value_{E1,Gx}, Value_{E2,Gx}, \ldots, Value_{En,Gx}\right) \quad (9)$$

$$GRcv = \frac{stddev(MR_{G1}, MR_{G2}, MR_{G3})}{mean(MR_{G1}, MR_{G2}, MR_{G3})} * 100 \quad (10)$$

where MV_{Gx} is the mean parameter value for genotype x (Gx) for environments 1 to n (E1…En), and MR_{Gx} is the mean of rankings of Gx in each environment.

4. RESULTS

4.1. Environmental characterisation

Figure 2 illustrates the time course of incident global radiation (SRAD, MJ/m^2), TT, WSI and PTQ values for each E.

Table A-3 (Supplementary Online Material) summarises key E parameters over three growth phases – germination, tillering and stalk growth, where the phases are determined by the Canegro1 model's standard parameter values for TT_EM50 and TT_OSG.

The warmest site was La Mare (seasonal cumulative TT10 ≈ 5400 °Cd), while the coolest was Pongola (≈ 4500 °Cd). La Mare P and R1 and Chiredzi P experienced warm conditions at the crop start, with cooler conditions later on; the other crops were started at a cooler time of year (Figure 2).

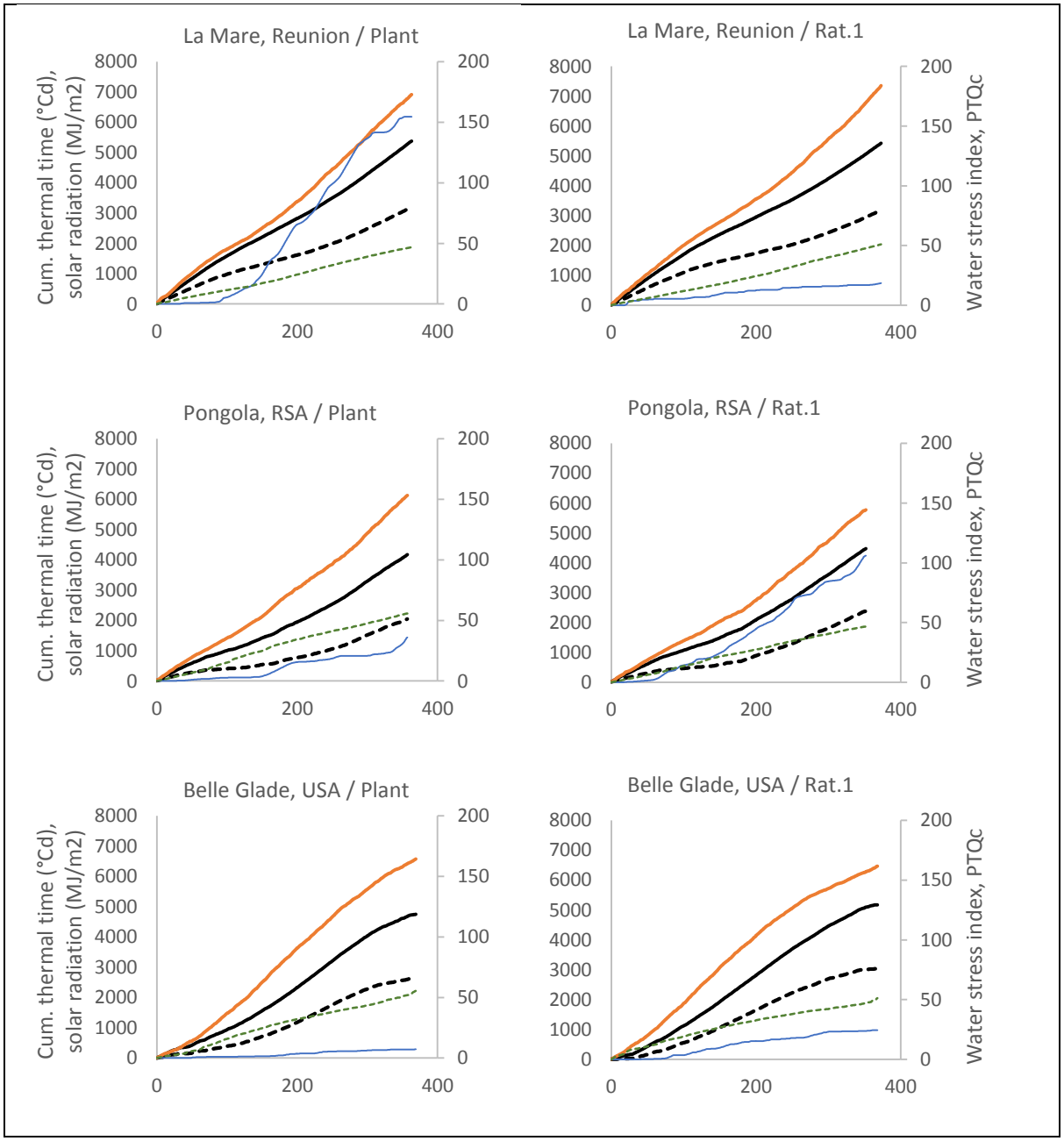
La Mare, Reunion / Plant
La Mare, Reunion / Rat.1
Pongola, RSA / Plant
Pongola, RSA / Rat.1
Belle Glade, USA / Plant
Belle Glade, USA / Rat.1
Cum. thermal time (°Cd), solar radiation (MJ/m2)
Water stress index, PTQc
0
1000
2000
3000
4000
5000
6000
7000
8000
0
50
100
150
200
0
200
400

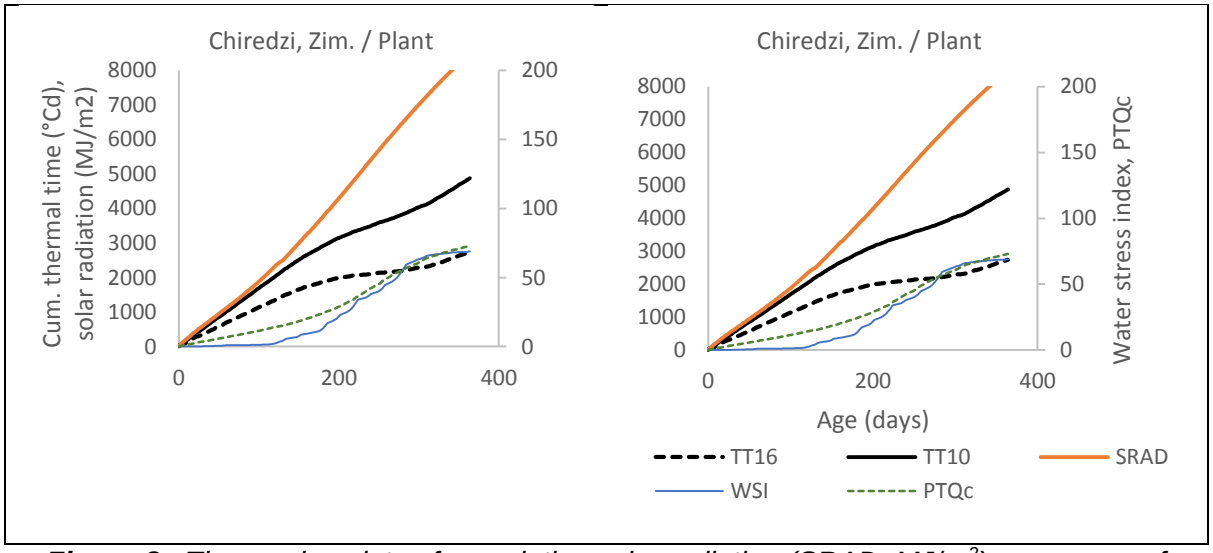

***Figure 2**. Time series plots of cumulative solar radiation (SRAD, MJ/m^2), measures of thermal time accumulation (TT16 and TT10), cumulative water stress index (WSI) and cumulative photo-thermal quotient (PTQc, divided by 10), for each Experiment.*

La Mare had the smallest temperature variation of all sites (all days averaged 16-30 °C, TMIN > 16 °C and TMAX < 35 °C). Chiredzi experienced the strongest weather variation – there were on average 50 days where TMIN < 10 °C and 64 days per year where TMAX > 35 °C. Despite being the coolest overall, Pongola still had significant numbers of hot (TMAX > 30 °C) and very hot (TMAX > 35 °C) days.

Chiredzi had the highest seasonal SRAD, with the P and R1 crops receiving 8477 and 7400 MJ/m^2 respectively. La Mare ranked second (7320 and 6914 MJ/m^2), Belle Glade third (6573 and 6456 MJ/m^2), and Pongola last (6132 and 5770 MJ/m^2).

The data in Figure 2 show that SRAD and TT accumulation had a similar relationship throughout the season at La Mare P and R1, and Pongola R1. Pongola P, Belle Glade P and R1 and Chiredzi R1 PTQc data suggest a high radiation to temperature ratio during the tillering phase for these Es (Table A-3), while the converse is true for the germination and tillering stages of Chiredzi P.

Pongola R1 experienced water stress through most of the growing period (seasonal average WSI=0.3) due to irrigation water use restrictions, while La Mare P and Chiredzi P were water stressed for most of the stalk growth phase with seasonal average WSI of 0.42 and 0.19 respectively (Figure 2 and Table A-3). These three Es were therefore considered water stressed. Other Es experienced relatively little water stress (WSI ≤ 0.1) through most of the growing period (Figure 2 and Table A-3) and were considered well-watered.

Biotic limitations were noted for some of the Es. Lodging was recorded at Pongola P, Belle Glade P, and Chiredzi P. The Belle Glade P crop experienced a frost event 38 days after planting, which affected only Q183. Brown and Tawny rust, Sesamia stalk borer, rats and rabbits affected cultivar HoCP96-540 at Belle Glade and Pongola. We believe these had little impact on outcomes, as we focussed mainly on the common Gs (generally ruling-out issues with Q183 and HoCP96-540) and unstressed experiments (so excluding Chiredzi P). Lodging recorded at Belle Glade P and Pongola P (along with drying-off at this site) may have led to reduced final ADM and SDM, but we believe this had little impact on the process-level analysis as the focus was seldom on final values.

4.2. Phenotypic characterisation

Observed phenotypic parameters (PPEAK, PFINAL, ADM and SDM at harvest), and derived phenotypic parameters based on modelling concepts, were calculated from the experimental data. These were then analysed for variation G and E, as well as GxE interactions via consistency of G rankings across Es.

The derived parameters allowed us to assess the extent to which model concepts explained the observations. In principle:

- strong variation with E indicates model concept shortcomings relating to simulating E effects.
- strong variation with G, and consistent G rankings – according to the significance criteria described in Section 4.3.3 - indicate G control over the related plant process(es) (and a need for G-specific parameters in models);
- strong variation with G and/or E, but with inconsistent G rankings, indicates unresolved GxE interaction effects.

Variation in parameter values across E and G for common Gs (N41, R570 and CP88-1762) is summarised in Table 3. Actual parameter values and correlation between parameters are provided in the Supplementary Online Material.

Results are presented for parameters relating to canopy development, then biomass accumulation and partitioning.

Table 3. *Coefficient of variance (%) of derived phenotypic parameter values. G indicates variation in mean values across three cultivars (N41, R570 and CP88-1762); E indicates variation in mean values across experiments (all, unstressed and stressed experiments). Mean rankings and cv% of rankings for unstressed Es are shown.*

	Unstressed Es								All Es		Stressed Es	
					Rankings							
	Mean value	**Units**	**E cv%**	**G cv%**	**N41**	**R570**	**CP88 -1762**	**G Rank cv%**	**E cv%**	**G cv%**	**E cv%**	**G cv%**
Parameter	**Derived parameters**											
TT_EM50 (P crops)	419	°Cd	34.2	10.5	1.5	2.0	2.5	25.0	31.3	5.3	36.5	1.7
TT_EM50 (R1 crops)	345	°Cd	39.4	37.8	1.7	2.7	1.7	28.9	41.3	32.1	-	4.9
PI	138	°Cd/leaf	15.5	8.7	1.6	3.0	1.4	43.6	13.5	8.4	5.0	7.5
TAR	0.027	shoots/m^2/°Cd	51.6	16.4	2.4	2.0	1.6	20.0	54.1	18.6	61.1	24.9
TT_Fi50	352	°Cd	19.8	10.3	2.5	2.3	1.3	33.1	25.2	10.0	18.1	10.8
RUEo	3.11	g/MJ	18.8	6.9	1.5	2.0	2.5	25.0	21.2	6.4	27.7	20.7
ADM_OSG	5.3	t/ha	80.4	10.8	2.2	2.2	1.6	17.3	82.8	4.6	93.2	45.2
TT_OSG	911	°Cd	39.2	6.9	2.6	2.0	1.4	30.0	44.5	3.2	50.6	8.7
STKPF	0.80	t/t	9.3	2.3	2.6	1.8	1.6	26.5	14.1	3.8	20.8	11.9
STKPF**	0.83	t/t	2.8	1.6	2.3	2.0	1.8	12.5	14.0	4.4	21.0	11.8
	Observed parameters											
PPEAK	21	shoots/m2	28.1	26.4	2.8	1.5	1.8	33.1	29.4	23.6	38.4	19.8
PFINAL	11	stalks/m2	34.6	17.6	2.4	1.2	2.4	34.6	36.3	17.8	42.3	19.2
ADM	49.4	t/ha	20.4	4.6	1.8	1.8	2.4	17.3	18.7	4.0	18.4	3.7
SDM	35.6	t/ha	15.8	6.4	2.0	1.6	2.4	20.0	16.9	9.6	4.8	16.5

**La Mare R1 excluded.

[A]TT10

[B]TT16

4.2.1. Canopy components

For P crops, mean TT_EM50 was similar to the default value for Canegro1 (428 °Cd), ≈50% lower than the Apsim default, and considerably greater than the Mosicas default parameter value, in equivalent TT terms. For ratoon crops, average TT_EM50 was greater than the equivalent default parameter values for Canegro1, Apsim and Mosicas.

TT_EM50 values were lowest for Pongola and highest for Chiredzi. Strong G variation combined with consistent G rankings (high GRcv) suggest significant G effects, with minimal GxE interaction effects, for P crops.

For R1 crops, E variation in TT_EM50 was slightly greater than that of P crops and exceeded the 25% threshold, indicating strong E effects, and hence an insufficient explanation of shoot emergence with thermal time. G variation was considerably higher than that of P crops, and rankings indicate that R570 consistently requires more TT for germination than other Gs. R570 required 619 °Cd for germination at Belle Glade R1, compared with ≈150 °Cd for other Gs in this E. R570 also required nearly 50% more TT for germination for Chiredzi R1 compared to N41 and CP88-1762, and about 30% more for Belle Glade P

E and G variation in PPEAK and PFINAL were considerable, but there was little GxE interaction as rankings were mostly consistent across the Es. Water stress affected the E averages, but had little effect on G rankings. PPEAK was consistently greater for unstressed than stressed crops.

TAR appears to be affected by both E and G factors. For the three common Gs, there was considerable variation in E (0.007-0.047 shoots/m^2/°Cd) and the cv was second-

highest of all parameters (52%). G rankings were relatively inconsistent (GRcv = 20%), suggesting the possible existence of GxE interaction effects. We note however that N41 had the highest TAR in six of eight Es, and CP88-1762 had the lowest in five Es.

E and G variation in PI was low, suggesting that E does not affect PI. Gcv for PI exceed our threshold for strong G effects, and the GRcv% value indicates that the G rankings are consistent for the three common Gs under unstressed conditions. R570 had the greatest PI in all five unstressed Es, while rankings (and average leaf PI values) were nearly identical for N41 and CP88-1762**.**

Relatively low E variation in TT_Fi50 suggests that canopy development is predominantly TT-driven. Further investigations (results not shown) also suggest that TT_Fi50 is more accurately modelled using TT16 than TT9, as E variation was lower with TT16. TT_Fi50 was smallest for CP88-1762 in five (out of seven) Es, and greatest for N41 in five Es. It should be noted that the underlying FIPAR observations used for these analyses were not always ideal in terms of quantity and quality, thereby reducing the confidence of these findings.

4.2.2. Biomass accumulation and partitioning

ADM at final harvest (Figure 3, Table A-10, Supplementary Online Material) ranged between 33.4 t/ha (R570 at Pongola, R1) and 71.2 t/ha (R570, La Mare, R1). SDM (Figure 4, Table A-10) was lowest for R570 at Pongola R1 (22.9 t/ha) and highest at Belle Glade P (52.2 t/ha). For the three Gs common to all Es, ANOVA results (Table A-4) indicate significant E ($p<0.001$) and GxE interaction ($p<0.01$) effects for ADM, for all Es and non-stressed Es only. SDM variances were significantly explained by E

(p<0.001), G (p<0.05 across all Es, p<0.1 for unstressed Es) and GxE interaction effects (p<0.01). SDM values at final harvest are shown in Figure 4.

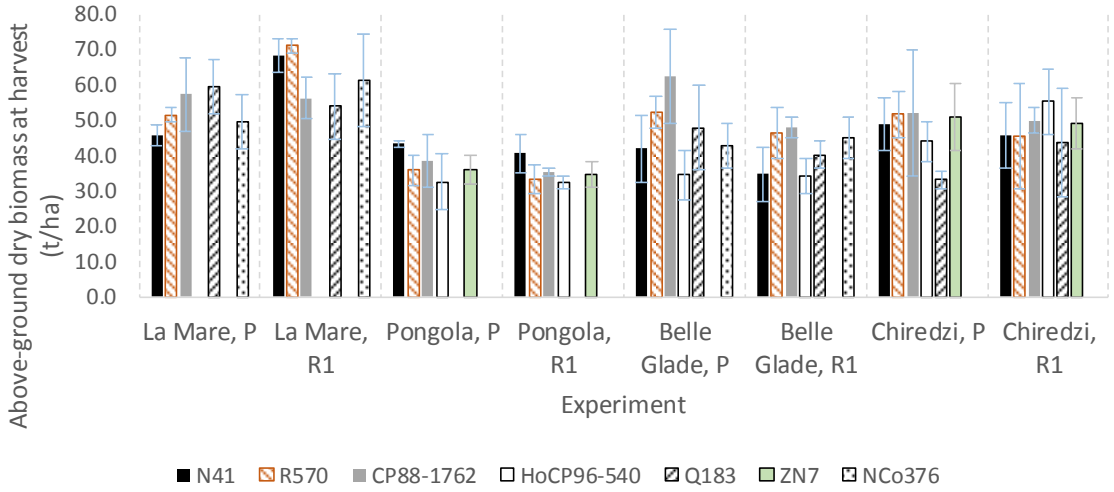

Figure 3. *Above-ground dry biomass at harvest for different cultivars and experiments. Error bars indicate one standard deviation of the mean.*

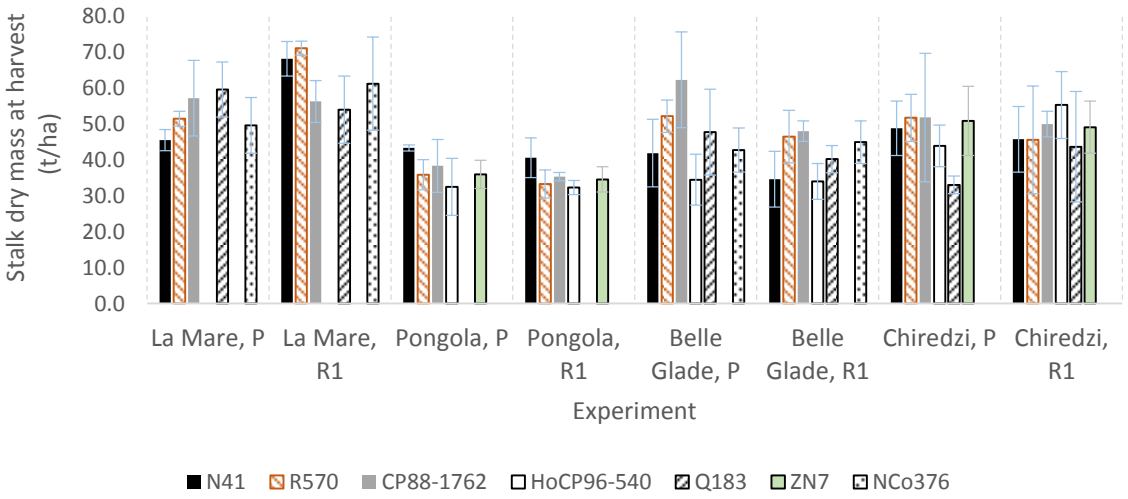

Figure 4. *Stalk dry mass at harvest for different cultivars and experiments. Error bars indicate one standard deviation of the mean.*

Average unstressed maximum RUE values are similar to the RUEmax parameters for the Apsim (equivalent to 3.3-3.6 g/MJ PAR) and Canegro1 and Canegro2 models (2.9-

3.4 g/MJ). RUEo values were consistent across Es (except for Chiredzi P, attributed to errors in estimating FiPAR for this experiment) with low E variation (Table 3).

The Es which best matched the predefined experimental conditions (fully irrigated ratoon crops with sufficient FiPAR data for the same set of five Gs) were the La Mare R1 and Belle Glade R1. For these Es the G-specific RUEo values were highly consistent and the G rankings were identical (Table 4).

Table 4. *Maximum sampling-period radiation use efficiency values (g/MJ intercepted PAR), and rankings, by Experiment and Cultivar, for the two most comparable experiments.*

Experiment	N41	R570	CP88-1762	HoCP96-540	Q183	ZN7	NCo376	Avg
	Values (g/MJ)							
La Mare, R1	3.11	3.17	3.18		2.57		2.69	2.94
Belle Glade, R1	3.35	3.48	4.28		2.57		3.20	3.38
All	3.23	3.33	3.73		2.57		2.95	3.16
	Rankings							
La Mare, R1	3.0	2.0	1.0		5.0		4.0	2
Belle Glade, R1	3.0	2.0	1.0		5.0		4.0	1
All	3.0	2.0	1.0		5.0		4.0	

The average value for ADM_OSG in this study was 5.3 t/ha and E variation was extremely high, for unstressed and stressed Es. G variation was strong and G rankings not consistent, indicating considerable GxE interaction. There were no clear crop class differences.

E variation in TT_OSG was half that of ADM_OSG, but still high (Table 3). G variation was very low, although CP88-1762 had a consistently lower TT_OSG than N41 and R570 (and rankings were fairly consistent, GRcv = 30%, indicating minimal GxE

interaction effects). Average TT_OSG for the common Gs was 1029 °Cd overall, 911 °Cd for non-stressed Es and 1226 °Cd for stressed Es.

E and G variation in STKPF (Table 3) were below our threshold values, indicating insufficient evidence of strong E and G effects for non-stressed Es and common Gs. It should be noted that the La Mare R1 crop values were unusually low compared to the other non-stressed Es, indicating possible sampling error. With this E omitted, STKPF values had even lower E variation. CP88-1762 ranked lowest in STKPF (of the three common Gs) in three unstressed Es, but ranked highest in one unstressed E. E and particularly G variation were considerably higher with stressed Es, and CP88-1762 had the highest STKPF of the common Gs for all three stressed Es.

5. DISCUSSION

Key findings are stated as bullet points, with the supporting discussion following.

5.1. Canopy development and light interception

5.1.1. Germination is strongly E- and G-controlled with little GxE interaction; for P crops, strong E variation in TT_EM50 indicates that E drivers in addition to TT influence time to primary shoot emergence, warranting further investigation.

Correct prediction of TT_EM50 is important: for P crops, it is correlated ($p<0.005$) with ADM and SDM (Table A-5, Supplementary Online Material); and several other derived parameters are defined in TT terms after emergence, potentially affecting their estimation accuracy.

Germination is presumably driven by soil temperature rather than air temperature, although all models considered use air temperature (probably for pragmatic reasons, that air temperature is available as an input, and soil temperature is not) to drive this process. Seasonal trends in soil temperatures tend to lag behind those in air temperatures. P crops are more likely to be affected by soil temperature dynamics because the buds are more deeply buried than with ratoon crops. The La Mare and Pongola P crops were started in late summer / early autumn, when soils might be expected to be warmer than the air, thus requiring less thermal time (in air temperature terms) for germination; this is reflected in the data with smaller TT_EM50 requirements. The Belle Glade and Chiredzi P crops were started in winter/spring, where soil temperatures would have been cooler than air temperatures and hence would be expected to require additional TT (based on air temperature) to achieve germination; this is borne out in the data, as these crops had higher TT_EM50 requirements. This pattern is less clear with ratoon crops. Soil temperature can be estimated from air temperature, incident radiation, canopy cover and soil albedo, and it is recommended that this approach be explored for improving the simulation of germination. Another possibility is that seedcane quality affected germination rates at the different sites.

5.1.2. Base temperatures used to calculate thermal time for germination are likely to be G-specific.

TT_EM50 values were noticeably greater for R570 than the other common Gs in some Es (Table A-6, Supplementary Online Material). An explanation for this could be that this cultivar has a higher base temperature requirement for germination. Belle Glade (P and R1) and Chiredzi P experienced much lower

average (16-18 °C) and minimum (TMIN ≈ 9-13 °C) temperatures during the germination period compared to the other sites (average daily temperature ≈ 22-28 °C, TMIN ≈ 16-24 °C), and had substantially greater TT_EM50 values for R570 than other Gs in these experiments. This is consistent with the findings of Poser et al. (2019), who reported a significantly higher germination T_B (13.3 °C) for R570 than two other cultivars tested. Similarly, Smit (2010) found different T_B values for germination for three cultivars (NCo376, N16 and N27).

5.1.3. There is significant G and E control over tillering/shoot population traits, and thermal time alone is not sufficient to predict shoot population under unstressed conditions.

The TAR value of 0.027 shoots/m^2/°Cd is considerably greater than the 0.0074 shoots/m^2/°Cd reported by Bezuidenhout et al. (2003). G differences in tillering rates have been reported in at least two other studies (Inman-Bamber, 1994; Singels et al., 2005b).

TAR appears to be affected by both E and G factors. For the three common Gs, there was considerable variation in E (Table 3). We note however that N41 had the highest TAR in six of eight Es, and CP88-1762 had the lowest in five Es. On balance, we interpret this as indicating a need for G-specific tillering parameters in models.

Unstressed tiller development has historically been considered to be driven solely by TT accumulation (Bezuidenhout et al., 2003; Keating et al., 1999; Singels, 2013; Singels et al., 2005b). However, the large E variation in TAR challenges this theory.

TAR decreased with increasing mean daily SRAD over the tillering period, although this relationship for non-stressed crops was not significant ($p = 0.08$)

(Figure 5). This concept should be explored further for possible inclusion in sugarcane crop models to improve simulation of POPN.

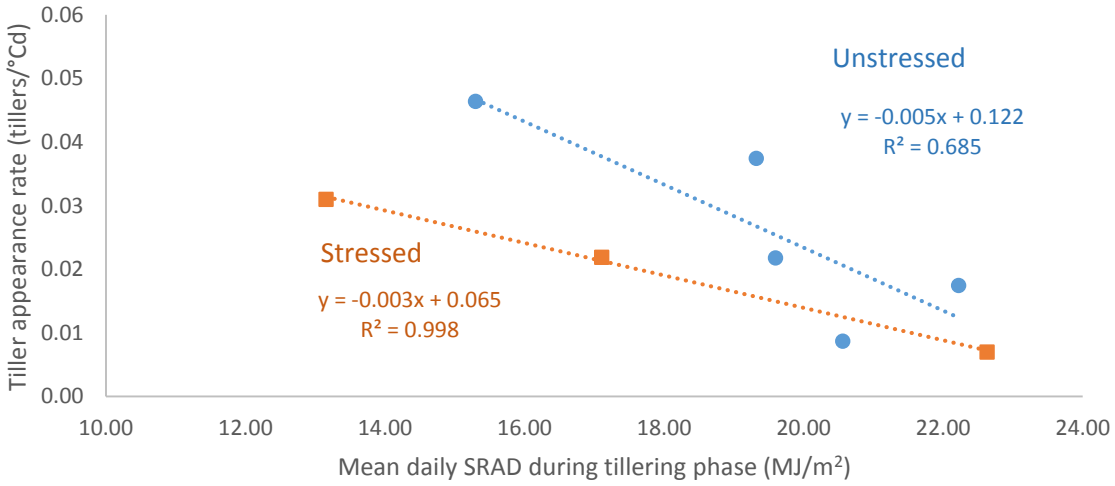

***Figure 5**. Relationship between mean tiller appearance rate and mean daily solar radiation (SRAD, MJ/m^2/d) for the tillering period, for non-stressed (filled circles) and stressed (filled squares) crops.*

5.1.4. PI is strongly G-controlled with minimal E and GxE interaction influences.

PI values determined in the study are comparable to values reported by Sinclair et al. (2004) for CP88-1762, Inman-Bamber (1994) and Bonnet (1998). Ecv was low and Gcv and GRcv were high. There is also much evidence in the literature for G-specific PIs (e.g. Bonnett, 1998; Inman-Bamber, 1994).

5.1.5. Canopy development rate is G-specific

G variation in TT_Fi50 for the common Gs is considered strong, and the rankings were sufficiently consistent (relatively high GRcv) to indicate G control over this trait.

5.2. Biomass accumulation and partitioning

5.2.1. Crop growth response differences to environmental factors is genotype-specific.

Differences in average ADM between Es were significant (Table A-4) and could be linked to climatic parameters. For example, La Mare R1 (highest ADM of the unstressed Es, 65.3 t/ha for the common Gs) had 38% greater TT10 and 20% greater SRAD than Pongola P (lowest ADM of unstressed Es for common Gs, 37.3 t/ha). Canopy development therefore occurred more rapidly and intercepted more incoming radiation for La Mare R1 than Pongola P (Table 3). La Mare R1 also had a higher average RUEmax than Pongola P (Table A-10), probably due to a more favourable temperature regime (24.8 compared to 21.7 °C, Table A-3)

GxE interaction in ADM was significant (Table A-4) and G rankings changed with E. For example N41 yielded higher than CP88-1762 in La Mare R1, but yielded lower in Belle Glade R1 (Table A-9, Supplementary Online Material). This coincided with a slightly higher and lower FIPARavg for N41 in La Mare R1 and Belle Glade R1 respectively (Table A-10). N41 also showed a much lower RUEmax than CP88-1762 in Belle Glade R1 (Table A-10). A notable difference between these Es is the average range in daily temperature, with Belle Glade R1 at 10.3 compared to 7.4 °C for La Mare R1 (Table A-3). CP88-1762 may be better adapted to the larger temperature range than N41.

G variance in SDM was statistically significant (Table A-4). CP88-1762 yielded highest for unstressed Es and common Gs) and N41 lowest. This coincided

with a higher RUEmax (Table A-10), a quicker canopy (TT_Fi50, Table A-5) and earlier OSG (TT_OSG, Table A-5).

5.2.2. Genotypic differences in RUEo are consistent over Es.

RUEmax showed moderate G variation for common Gs at unstressed Es, and very consistent G rankings over Es. The identical rankings of RUEmax for five Gs at Belle Glade and La Mare are remarkable, considering that these sites are 15 000 km apart, with completely different soils, start dates, irrigation methods, biotic stresses and numerous other differences. The similarity is striking and strongly suggests that RUEo is G-specific and stable across Es. Hoffman et al. (2018) and Marin et al. (2011) reported G differences in RUEmax.

5.2.3. TT_OSG is recommended over ADM_OSG as a simulation approach for crop models, and it is clear that TT or ADM alone are insufficient for predicting OSG.

Ecv for ADM_OSG was approximately double that of TT_OSG. Further testing with complete models is however necessary to assess this in combination with a variable STKPF, as in the Mosicas model. Water stress should also be taken into account when predicting OSG. The evidence from this study is inconclusive regarding the extent to which this trait is also G-controlled.

Results indicate that TT accumulation (under non-limiting water conditions) does not sufficiently account for E differences in OSG. Characterising related G differences (and resolving GxE interaction effects) may only be possible once the E drivers of these processes are better understood. The relationship between mean TT_OSG and mean daily SRAD over the tillering period is robust ($R^2 \approx 0.70$, $p<0.05$), and holds for stressed and irrigated crops (Figure 6). This

suggests that TT_OSG is lower when SRAD is higher. This needs to be investigated further to more fully elucidate the underlying mechanisms.

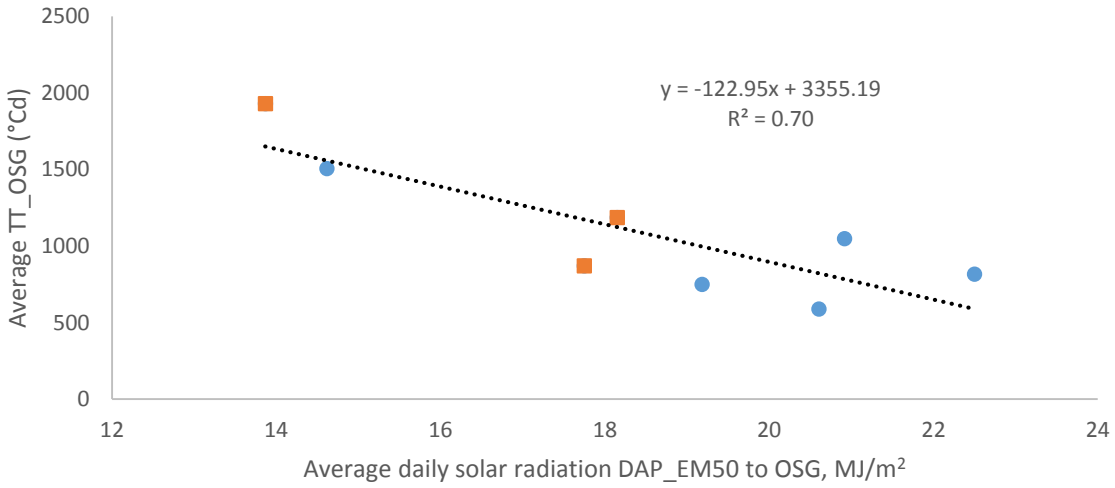

Figure 6. *Relationship between thermal time (TT10) from emergence to start of stalk growth averaged over cultivars and average daily incident shortwave radiation for the different experiments. Higher-intensity radiation per unit thermal time appears to result in earlier onset of stalk elongation. Water-stressed experiments are shown as filled squares. The linear trend lines were fitted to all data points (stressed and non-stressed combined).*

It is surmised that OSG (and the end of the tillering period as indicated by PPEAK) is a response to competition for light. More profuse tillering under relatively sunny conditions, as found in sorghum (Kim et al., 2010), may lead to earlier OSG as a response to competition for light (supported by significant correlation between TT_OSG and TAR found in our study). Tiller senescence is triggered by the radiation environment in many crops (red to far-red radiation ratio, e.g. Lafarge and Hammer (2002)). Tillering in sugarcane has been reported to cease at 70% FiPAR (Inman-Bamber, 1994), and at 90% intra-row

FiPAR (Singels and Smit, 2009). These thresholds may be G-specific, with values reported from 55% (ZN7) to 75% (N14) (Singels et al., 2005b; Zhou et al., 2003). Bezuidenhout et al. (2003) suggested that tiller senescence due to light competition starts later in subsequent ratoons due to stool widening. Allison et al. (2007) found that rapid stalk growth began at PPEAK in irrigated sugarcane and Napier grass.

It is not clear whether it is necessary to simulate a gradual transition from tillering to stalk elongation based on phenological development of shoot cohorts of different thermal age; doing so may achieve better simulation of low level leaf and tiller trait impacts on crop performance.

5.2.4. Under well-watered conditions, STKPF is a robust parameter, unlikely to change by G or E, for the Gs tested here.

The small observed G variation in STKPF is not agreement with current thinking represented in models, which allow for G-specific values for related model parameters. Hoffman et al. (2018) found statistically significant differences in stalk fraction in an irrigated pot trial, although the range of values was narrow. In an Apsim model parameter sensitivity analysis for two environments in Australia (Sexton et al., 2017), 10 model parameters were ranked according to their influence in determining simulated yields (where 1st-ranked was the most influential and 10th-ranked the least); STKPF ranked sixth for biomass yields eighth for sucrose yields. The Apsim model does however have the same value (0.70 t/t) for the vast majority of standard cultivar definitions. There is a possibility of a G-specific STKPF response to water stress, also not reflected in any of the models considered.

5.3. Process-level evaluation of crop model concepts

We believe that the approach demonstrated in this study of analysing crop growth in terms of process-level concepts from crop models is enormously valuable for improving crop modelling for supporting breeding applications. Many of the phenotypic parameters quantified can be used directly or indirectly as model input parameter values. Shortcomings in crop models, particularly situations where errors in one process compensate for errors in other processes, will be highlighted by constraining the number and value range of parameters that can be determined via trial and error. Correcting these will ensure that models operate more realistically in terms of process composition. This supports one of the key tenets of crop model suitability for crop improvement, that models emulate of the biology of the plant.

5.4. Significance of the international multi-genotype, multi-environment dataset

Relatively few sugarcane 'multi-environment trials' (METs) have been conducted, and all such trials that we are aware of have been conducted in a single country. While considerable E diversity can exist in a single country, we believe that the dataset described here offers considerable additional value by spanning very different growing environments. The cultivars grown are similarly diverse, originating from different breeding programmes, with different objectives and germplasm pedigrees. Finally, this is a growth analysis- rather than breeding-focussed dataset, which provides not only the opportunity to characterise G, E and GxE interaction effects, but also attempts to understand and explain these at a process level. This offers possibilities for improvement to the fundamental mechanisms of process-based sugarcane models,

which simultaneously improves the models for more effective application in crop improvement activities by (further) unravelling genotypic control over complex traits, as well as generally improving the accuracy of the models for more 'traditional' applications, such as yield benchmarking, forecasting and irrigation scheduling.

6. CONCLUSION

Growth analysis data from an international multi-environment trial were used to gain a better understanding of G and E effects on biomass production and stalk yields. Above-ground dry biomass (ADM) and stalk dry mass (SDM) yields at final harvest showed significant E and GxE variation. Notable traits of the three common Gs include: rapid tillering, high peak and final shoot population for N41; slow leaf appearance rate and low shoot population with R570; and rapid canopy development and high radiation use efficiency for CP88-1762.

Main findings include:

- Significant E variation was observed for phenotypic parameters TT_EM50 (thermal time (TT) to 50% primary shoot emergence), TAR (tiller appearance rate per unit TT) and TT_OSG (TT from 50% primary shoot emergence to onset of stalk elongation (OSG)). This challenges (1) the use of air temperature to drive shoot emergence, where simulated soil temperature is proposed as an alternative; and (2) the use of TT as the sole driver of unstressed tillering rate and OSG timing, where solar radiation was found to have a significant influence on these (in addition to TT). OSG timing also appears to be affected by water stress.

- Significant G variation was observed for TT requirements for leaf and canopy development, and RUEo, with little E variation in these. Stalk partitioning fraction was found to vary very little between G or E.
- Determining the date of primary shoot emergence accurately was both challenging and important, as many crop timing parameters are defined with reference to this phenological event.

By explaining more of the E variation, more stable and accurate G-specific model parameters can be defined and evaluated. This is anticipated to lead to less GxE confounding of modelled processes, and hence crop models that are better-equipped for supporting sugarcane crop improvement activities.

Crop model concepts have been explored in this work. The next step is to assess the crop models themselves in terms of their abilities to simulate GxE interactions at these sites. Following that – as necessary – model refinements, addressing some of the weaknesses (and their possible solutions) identified in this paper, will be implemented and tested.

ACKNOWLEDGEMENTS

The authors would like gratefully to acknowledge

- Maurits van den Berg and Michiel Smit who conceived and developed the idea for generating this international growth analysis data set,
- funding from the International Consortium for Sugarcane Modelling (and participating research organizations),

- technical assistance with and infrastructure support for experimental work from participating research organizations,
- helpful suggestions for paper improvement from two anonymous reviewers.

REFERENCES

Allison, J.C.S., Pammenter, N.W., Haslam, R.J., 2007. Why does sugarcane (Saccharum sp. hybrid) grow slowly? South African J. Bot. 73, 546–551. https://doi.org/10.1016/j.sajb.2007.04.065

Bezuidenhout, C.N., O'Leary, G.J., Singels, A., Bajic, V.B., 2003. A process-based model to simulate changes in tiller density and light interception of sugarcane crops. Agric. Syst. 76, 589–599. https://doi.org/10.1016/S0308-521X(02)00076-8

Bonnett, G.D., 1998. Rate of leaf appearance in sugarcane, including a comparison of a range of varieties. Funct. Plant Biol. 25, 829–834.

Boote, K., Jones, J., Hoogenboom, G., White, J. (2010). The Role of Crop Systems Simulation in Agriculture and Environment. Int. J. Agric. Env. Info. Sys. (IJAEIS), 1(1), 41-54. doi:10.4018/jaeis.2010101303

Hammer, G.L., Jordan, D.R., 2007. An integrated systems approach to crop improvement., in: Sadras, V., Calderini, D. (Eds.), Scale and Complexity in Plant Systems Research: Gene-Plant-Crop Relations. Springer-Verlag GmbH, Heidelberg, pp. 45–61.

Hoffman, N., Singels, A., Patton, A., Ramburan, S., 2018. Predicting genotypic differences in irrigated sugarcane yield using the Canegro model and independent trait parameter estimates. Eur. J. Agron. 96, 13–21.

https://doi.org/https://doi.org/10.1016/j.eja.2018.01.005

Inman-Bamber, N.G., 1994. Temperature and seasonal effects on canopy development and light interception of sugarcane. Field Crop. Res. 36, 41–51. https://doi.org/10.1016/0378-4290(94)90051-5

Inman-Bamber, N.G., 1991. A growth model for sugar-cane based on a simple carbon balance and the CERES-Maize water balance. South African J. Plant Soil 1862, 37–41. https://doi.org/10.1080/02571862.1991.10634587

Inman-Bamber, N.G., Jackson, P.A., Stokes, C.J., Verrall, S., Lakshmanan, P., Basnayake, J., 2016. Sugarcane for water-limited environments: Enhanced capability of the APSIM sugarcane model for assessing traits for transpiration efficiency and root water supply. Field Crop. Res. 196, 112–123. https://doi.org/10.1016/j.fcr.2016.06.013

Jones, M.R., Singels, A., 2018. Refining the Canegro model for improved simulation of climate change impacts on sugarcane. Eur. J. Agron. https://doi.org/10.1016/j.eja.2017.12.009

Jones, M.R., Singels, A., Thorburn, P., Marin, F., Martine, J.F., Chinorumba, S., Viator, R., Nunez, O., 2014. Evaluation of the DSSAT-Canegro model for simulating climate change impacts at sites in seven countries. Proc. S. Afr. Sugar Technol. Assoc. 87, 323–329.

Jones, M., Singels, A., Inman-Bamber, N., 2011. Simulating Source and Sink Control of Structural Growth and Development and Sugar Accumulation in Sugarcane. Proc S Afr Sug Technol Ass 84, 157–163.Keating, B.A., Robertson, M.J., Muchow, R.C., Huth, N.I., 1999. Modelling sugarcane production systems I.

Development and performance of the sugarcane module. Field Crop. Res. 61, 253–271. https://doi.org/10.1016/S0378-4290(98)00167-1

Kim, H.K., Oosterom, E. van, Dingkuhn, M., Luquet, D., Hammer, G., 2010. Regulation of tillering in sorghum: environmental effects. Ann. Bot. 106, 57–67. https://doi.org/10.1093/aob/mcq079

Lafarge, T.A., Hammer, G.L., 2002. Tillering in Grain Sorghum over a Wide Range of Population Densities: Modelling Dynamics of Tiller Fertility. Ann. Bot. 90, 99–110.

Marin, F.R., Jones, J.W., Royce, F., Suguitani, C., Donzeli, J.L., Pallone Filho, W.J., Nassif, D.S.P., 2011. Parameterization and evaluation of predictions of DSSAT/CANEGRO for Brazilian sugarcane. Agron. J. 103, 304–315.

Marin, F.R., Jones, J.W., Singels, A., Royce, F., Assad, E.D., Pellegrino, G.Q., Justino, F., 2013. Climate change impacts on sugarcane attainable yield in southern Brazil. Clim. Change 117, 227–239. https://doi.org/10.1007/s10584-012-0561-y

Marin, F.R., Thorburn, P.J., Nassif, D.S.P., Costa, L.G., 2015. Sugarcane model intercomparison: Structural differences and uncertainties under current and potential future climates. Environ. Model. Softw. 72, 372–386. https://doi.org/10.1016/j.envsoft.2015.02.019

Martiné, J.-F., Siband, P., Bonhomme, R., 1999. Simulation of the maximum yield of sugar cane at different altitudes: effect of temperature on the conversion of radiation into biomass. Agronomie 19, 3–12.

Martiné, J.-F., Todoroff, P.R.I., 2004. Le modèle de croissance mosicas et sa plateforme de simulation simulex: état des lieux et perspectives. Rev. Agric. Sucrière l'Ile Maurice 80 LB-U1, 133–147.

Mebane, W.R., Sekhon, J.S., 2011. Genetic Optimization Using Derivatives: The {rgenoud} Package for {R}. J. Stat. Softw. 42, 1–26.

Ngobese, I., Ramburan, S., Labuschagne, M., 2018. Quantifying sugarcane cultivar differences in tiller and stalk phenology: identifying traits suited to crop model-assisted breeding. J. Crop Improv. 32, 847–860. https://doi.org/10.1080/15427528.2018.1534762

Nix, H.A., 1976. Climate and crop productivity in Australia. Int. Rice Res. Inst. Clim. rice.

Poser, C., Barau, L., Mezino, M., 2019. Effect of the emergence threshold temperature on the geographical distribution of a sugar cane variety.

R Core Team, 2016. R: A Language and Environment for Statistical Computing. Sexton, J., Everingham, Y.L., Inman-Bamber, G., 2017. A global sensitivity analysis of cultivar trait parameters in a sugarcane growth model for contrasting production environments in Queensland, Australia. Eur. J. Agron. 88, 96–105. https://doi.org/10.1016/j.eja.2015.11.009

Sinclair, T.R., Gilbert, R.A., Perdomo, R.E., Shine, J.M., Powell, G., Montes, G., 2004. Sugarcane leaf area development under field conditions in Florida, USA. Field Crop. Res. 88, 171–178. https://doi.org/10.1016/j.fcr.2003.12.005

Singels, A., 2013. Crop Models. Sugarcane Physiol. Biochem. Funct. Biol., Wiley Online Books. https://doi.org/doi:10.1002/9781118771280.ch20

Singels, A., Bezuidenhout, C.N., 2002. A new method of simulating dry matter partitioning in the Canegro sugarcane model. Field Crop. Res. 78, 151–164. https://doi.org/10.1016/S0378-4290(02)00118-1

Singels, A., Donaldson, R.A., 2000. A simple model of unstressed sugarcane canopy development. Proc. S. Afr. Sugar Technol. Assoc. 74, 151–154.

Singels, A., Donaldson, R.A., Smit, M.A., 2005a. Improving biomass production and partitioning in sugarcane: Theory and practice. Field Crop. Res. 92, 291–303. https://doi.org/10.1016/j.fcr.2005.01.022

Singels, A., Hoffman, N., Paraskevepoulos, A.L., Ramburan, S., 2016. Sugarcane genetic trait parameter estimation., in: Proceedings of the ICROPM2016 International Crop Modelling Symposium Held from 15 to 17 March 2016 in Berlin. pp. 143–144.

Singels, A., Inman-Bamber, N.G., 2011. Modelling genetic and environmental control of biomass partitioning at plant and phytomer level of sugarcane grown in controlled environments. Crop Pasture Sci. 62, 66–81. https://doi.org/10.1071/CP10182

Singels, A., Jones, M.R., Van den Berg, M., 2008. DSSAT v4.5 - Canegro Sugarcane Plant Module Scientific documentation. South African Sugarcane Research Institute.

Singels, A., Paraskevepoulos, A.L., 2017. The Canesim Sugarcane Model: Scientific Documentation. South African Sugarcane Research Institute.

Singels, A., Smit, M.A., 2009. Sugarcane response to row spacing-induced competition for light. Field Crop. Res. 113, 149–155. https://doi.org/10.1016/j.fcr.2009.04.015

Singels, A., Smit, M.A., Redshaw, K.A., Donaldson, R.A., 2005b. The effect of crop start date, crop class and cultivar on sugarcane canopy development and

radiation interception. Field Crop. Res. 92, 249–260. https://doi.org/10.1016/j.fcr.2005.01.028

Smit, M.A., 2010. Characterising the factors that affect germination and emergence in sugarcane. Proc. S. Afr. Sugar Technol. Assoc. 83, 230–234.

Thorburn, P., Biggs, J., Jones, M.R., Singels, A., Marin, F., Martine, J.F., Chinorumba, S., Viator, R., Nunez, O., 2014. Evaluation of the APSIM-Sugar model for simulating sugarcane yield at sites in seven countries: initial results. Proc. S. Afr. Sugar Technol. Assoc. 87, 318–322.

van Dillewijn, C., 1952. Botany of Sugarcane. Chronica Botanica; New York: Stechert-Hafner.

Yin, X., Struik, P.C., Kropff, M.J., 2004. Role of crop physiology in predicting gene-to-phenotype relationships. Trends Plant Sci. 9, 426–432. https://doi.org/10.1016/j.tplants.2004.07.007

Zhou, M.M., Singels, A., Savage, M.J., 2003. Physiological parameters for modelling differences in canopy development between sugarcane cultivars. Proc. S. Afr. Sugar Technol. Assoc. 77, 610–621.